

The two-dimensional Heisenberg ferromagnet as an approach to adsorbed ^3He magnetism

This article has been downloaded from IOPscience. Please scroll down to see the full text article.

1990 J. Phys.: Condens. Matter 2 4161

(<http://iopscience.iop.org/0953-8984/2/18/013>)

View [the table of contents for this issue](#), or go to the [journal homepage](#) for more

Download details:

IP Address: 171.66.16.103

The article was downloaded on 11/05/2010 at 05:54

Please note that [terms and conditions apply](#).

The two-dimensional Heisenberg ferromagnet as an approach to adsorbed ^3He magnetism

Evandro V L de Mello and Mucio A Continentino

Departamento de Física, Universidade Federal Fluminense, Outeiro de S João Batista S/N, 24020 Niterói, RJ, Brazil

Received 5 October 1989

Abstract. Recent experiments have measured the magnetisation of one to three ^3He atomic layers adsorbed on graphite. The properties of this novel system were interpreted by a two-dimensional ferromagnetic Heisenberg model. We perform real-space renormalisation group calculations for the two-dimensional triangular Heisenberg model with a magnetic field. We also make a quantum mechanical generalisation of a method which calculates the magnetisation recursively at any point of the global phase diagram. Our theoretical results for $T > J = 2.1$ mK agree well with the experimental data and the exact high-temperature expansion. For $T < J$ the agreement with the data is only qualitative.

1. Introduction

The nuclear magnetic properties of solid ^3He have sparked off a large number of theoretical and experimental studies in the past 20 years. The two solid low-density distinct, magnetically ordered phases and other properties of liquid ^3He offers a unique opportunity to study fundamental problems of quantum mechanics [1]. The study of the magnetisation of ^3He films and its properties has also attracted considerable attention [2–4].

Most of the recent work on adsorbed ^3He involves exfoliated graphite as substrate because it is the best characterised system for surface studies and a close approximation to ideal two-dimensional systems [5, 6]. Lately the magnetism of ^3He up to three atomic layers was studied [7–9]. According to the current theoretical interpretation of the three-particle ring exchange mechanism for three-dimensional solid ^3He [1] and also adsorbed ^3He [10] the data were interpreted in the following way [11]: the high density of the first layer precludes any significant particle exchange and its magnetic properties are essentially described by a free-spin Curie law. The third-layer atoms form a degenerate Fermi fluid and therefore their magnetisation is very small. Most of the signal in the low-temperature (2 mK) regime is due to the second-layer atoms, which are able to perform quantum mechanical tunnelling motions. Furthermore a high-temperature expansion for the two-dimensional Heisenberg model reproduced very well the magnetisation data for $T > 2.1$ mK, and the low-temperature behaviour of the susceptibility was exponential like, in agreement with theoretical predictions [7, 11]. Thus it was conjectured that the adsorbed ^3He at millikelvin temperatures provides the first example of a real two-dimensional nuclear Heisenberg ferromagnet.

Motivated by this new two-dimensional Heisenberg system we generalise the quantum mechanical real space renormalisation group method of Caride *et al* [12] in order to deal with the Heisenberg model in the *presence of a magnetic field*. Our aim is to develop a technique that can be applied for any arbitrary temperature. This is not the case of the high-temperature expansion used in [7, 11] valid only for $T > J$ where J is the exchange interaction. However, the non-commutative quantum aspect of the system introduces discrepancies when it is treated ‘by pieces’ [13] as in the approximate renormalisation group procedures. Quantitative studies [14] have established that decomposition into subarray methods are strictly correct for classical systems and are an excellent approximation for all temperatures when applied to quantum systems. Comparison between a cluster renormalised as a whole and by ‘by pieces’ revealed differences of order of 10% for the renormalised coupling constant J in the low-temperature regime $T < J$ [14]. The present work is a first step in the calculation of the thermodynamic properties of the quantum Heisenberg model in an external field using real-space renormalisation group methods. Larger arrays which enable more reliable results to be obtained will be studied in the future.

The plan of the paper is as follows: the scaling method for the Heisenberg model in the presence of a magnetic field is developed in section 2. In section 3 we derive the quantum renormalisation group recursion relations, their flow and fixed points. We also obtain the low-temperature scaling properties and study the dynamic behaviour. In section 4 the generalised magnetisations are defined and it is shown how to obtain the measured magnetisation recursively. Section 5 contains the analysis of the renormalisation group equations, the comparison between our calculations and the experimental results of [7, 11]. We conclude in section 6 and discuss how improvements can be made upon our method.

2. Heisenberg model and formalism

Let us assume a two-dimensional crystal of N sites described by the reduced Hamiltonian

$$\mathcal{H} = \sum_{\langle ij \rangle} [W(\sigma_i^x \sigma_j^x + \sigma_i^y \sigma_j^y) + K\sigma_i^z \sigma_j^z] + H \sum_i \sigma_i^z + NC \quad (1)$$

where σ_i, σ_j are Pauli operators for neighbour sites whose components σ^x, σ^y and σ^z are the usual Pauli matrices associated with spin $\frac{1}{2}$ and where $K \equiv J/2k_B T$, $W \equiv J(1 - \Delta)/2k_B T$ and $H \equiv \mu B_0/k_B T$, B_0 being the applied external magnetic field taken in the z direction, μ the magnetic moment and C a constant which will be referred to later. The first sum is over a pair of neighbour sites only and the second is extended over the whole crystal.

For the kind of calculations that we are going to perform, it is convenient to rewrite (1) as a bond Hamiltonian;

$$\mathcal{H} = \sum_{\langle ij \rangle} \left(W(\sigma_i^x \sigma_j^x + \sigma_i^y \sigma_j^y) + K\sigma_i^z \sigma_j^z + \frac{H}{Z}(\sigma_i^z + \sigma_j^z) + \frac{2C}{Z} \right) \quad (2a)$$

$$\mathcal{H} = \sum_{\langle ij \rangle} \mathcal{H}_{ij} \quad (2b)$$

Z being the coordinate number.

The renormalisation group treatment used here consists of two basic steps.

(i) The first is bond shifting which leads to parallel arrays of two or more bonds. If we are dealing with n parallel bonds, they are simply replaced by their sum [14, 15].

(ii) The second step is a decimation which consists of taking the trace over the spin states of all internal sites of a given linear chain. Thus, for a chain with N internal sites,

$$\exp(\mathcal{H}'_{12}) = \text{Tr}_N[\exp(\mathcal{H}_{13} + \mathcal{H}_{34} + \dots + \mathcal{H}_{NZ})] \quad (3)$$

where

$$\mathcal{H}'_{12} = W'(\sigma_1^x \sigma_2^x + \sigma_1^y \sigma_2^y) + K' \sigma_1^z \sigma_2^z + (H'/Z)(\sigma_1^z + \sigma_2^z) + 2C'/Z \quad (4)$$

and Tr_N denotes the trace over states of the N internal spins. Equation (3) relates the renormalised parameters of H'_{12} to those of the initial chain Hamiltonian in such way as to maintain the same Boltzmann probabilities for the remaining spins.

These two steps are combined into a Migdal–Kadanoff renormalisation group method [14, 15] which is very convenient because no extension of parameter space is needed, so that the starting Hamiltonian transforms into one of the same form. The first step is trivial for any integer scaling factor b , but even for the simplest case of one internal site ($b = 2$) the second step is cumbersome because of non-commutativity properties. Next we show how to obtain the renormalisation group equations.

3. Recursion relations for $b = 2$

For the $b = 2$ case, equation (3) becomes

$$\exp(\mathcal{H}'_{12}) = \text{Tr}_{\{\sigma_3\}}[\exp(\mathcal{H}_{123})] \quad (5)$$

where

$$\mathcal{H}_{123} = W(\sigma_1^x \sigma_3^x + \sigma_1^y \sigma_3^y + \sigma_3^x \sigma_2^x + \sigma_3^y \sigma_2^y) + K(\sigma_1^z \sigma_3^z + \sigma_3^z \sigma_2^z) + (H/Z)(\sigma_1^z + 2\sigma_3^z + \sigma_2^z) + 4C/Z \quad (6)$$

and

$$\mathcal{H}'_{12} = W'(\sigma_1^x \sigma_2^x + \sigma_1^y \sigma_2^y) + K' \sigma_1^z \sigma_2^z + (H'/Z)(\sigma_1^z + \sigma_2^z) + 2C'/Z. \quad (7)$$

Note that the weight factor for the interactions with the field is a direct consequence of equations (2a) and (2b).

The expansion of $\exp(\mathcal{H}'_{12})$ yields

$$\exp(\mathcal{H}'_{12}) = a' + b'_{12}(\sigma_1^x \sigma_2^x + \sigma_1^y \sigma_2^y) + c'_{12} \sigma_1^z \sigma_2^z + d'_{12}(\sigma_1^z + \sigma_2^z) \quad (8)$$

where the coefficients a' , b' and c' depend on K' , W' , H' and C' . Similarly the expansion of $\exp(\mathcal{H}_{123})$ yields

$$\begin{aligned} \exp(\mathcal{H}_{123}) = & a + b_{13}(\sigma_1^x \sigma_3^x + \sigma_1^y \sigma_3^y) + b_{23}(\sigma_2^x \sigma_3^x + \sigma_2^y \sigma_3^y) + b_{12}(\sigma_1^x \sigma_2^x + \sigma_1^y \sigma_2^y) \\ & + c_{13} \sigma_1^z \sigma_3^z + c_{23} \sigma_2^z \sigma_3^z + c_{12} \sigma_1^z \sigma_2^z + d_{12}(\sigma_1^z + \sigma_2^z) + d_{33} \sigma_3^z \\ & + h_{123}[\sigma_1^z(\sigma_3^x \sigma_2^x + \sigma_3^y \sigma_2^y) + \sigma_2^z(\sigma_3^x \sigma_1^x + \sigma_3^y \sigma_1^y)] + f_{123} \sigma_1^z \sigma_2^z \sigma_3^z \end{aligned} \quad (9)$$

and again the coefficients of the expansion are functions of the parameters of \mathcal{H}_{123} . From equations (5), (8) and (9), it follows that

$$a' = 2a \quad (10a)$$

$$b'_{12} = 2b_{12} \quad (10b)$$

$$c'_{12} = 2c_{12} \quad (10c)$$

$$d'_{12} = 2d_{12}. \quad (10d)$$

Our task is to write the coefficients of the LHS in terms of W' , K' , H' and C' and those of the RHS in terms of W , K , H and C . Following along the lines described by Mariz *et al* [14], we derive

$$\exp(4H'/Z) = (a' + c'_{12} + 2d'_{12})/(a' + c'_{12} - 2d'_{12}) \quad (11a)$$

$$\exp(4W') = (a' - c'_{12} + 2b'_{12})/(a' - c'_{12} - 2b'_{12}) \quad (11b)$$

$$\exp(4K') = [(a' + c'_{12})^2 - 4d'^2_{12}]/[(a' - c'_{12})^2 - 4b'^2_{12}] \quad (11c)$$

and

$$\exp(2C'/Z) = (a' - c'_{12} - 2b'_{12})/\exp(-2W' - K'). \quad (11d)$$

Performing the same calculations for \mathcal{H}_{123} , we find that

$$a = \frac{1}{8} \left\{ \exp\left(4K + \frac{4C}{Z}\right) \left[\exp\left(\frac{8H}{Z}\right) + \exp\left(\frac{-8H}{Z}\right) \right] + \sum_{i=1}^3 \{ \exp[\varepsilon_i(H)] + \exp[\varepsilon_i(-H)] \} \right\} \quad (12a)$$

$$c_{12} = \frac{1}{4} \left\{ \exp\left(4K + \frac{4C}{Z}\right) \left[\exp\left(\frac{8H}{Z}\right) + \exp\left(\frac{-8H}{Z}\right) \right] + \sum_{i=1}^3 \{ \exp[\varepsilon_i(H)] \lambda_{1i}^2(H) + \exp[\varepsilon_i(-H)] \lambda_{1i}^2(-H) \} \right\} - a \quad (12b)$$

$$b_{12} = \frac{1}{4} \sum_{i=1}^3 \{ \exp[\varepsilon_i(H)] \lambda_{2i} \lambda_{3i}(H) + \exp[\varepsilon_i(-H)] \lambda_{2i} \lambda_{3i}(-H) \} \quad (12c)$$

and

$$d_{12} = \frac{1}{8} \left\{ \exp\left(4K + \frac{4C}{Z}\right) \left[\exp\left(\frac{8H}{Z}\right) - \exp\left(\frac{-8H}{Z}\right) \right] + \sum_{i=1}^3 \{ \exp[\varepsilon_i(H)] \lambda_{1i}^2(H) - \exp[\varepsilon_i(-H)] \lambda_{1i}^2(-H) \} \right\}. \quad (12d)$$

The variables ε and λ are eigenvalues and eigenvector components of the following matrix:

$$\mathbf{A}(\pm H) = \begin{bmatrix} -4K + 4C/Z & 4W & 4W \\ 4W & \pm 4H/Z + 4C/Z & 0 \\ 4W & 0 & \pm 4H/Z + 4C/Z \end{bmatrix}. \quad (13)$$

We have multiplied W , K , H and C by 2 in equations (12) and (13) because of the first step bond moving of the renormalisation group method. Applying the above results for the two-dimensional triangular ($Z = 6$) lattice we obtain the following renormalisation group recursion relations:

$$W' = \frac{1}{4} \ln \left\{ \exp(H/3) [\cosh(2\Delta_+) + \alpha_+/\Delta_+ \sinh(2\Delta_+)] + \exp(-H/3) [\cosh(2\Delta_-) + \alpha_-/\Delta_- \sinh(2\Delta_-)] \right\} / 2 \exp(2K) \cosh(2H/3) \quad (14a)$$

$$\begin{aligned}
 K' = \frac{1}{4} \ln & \left\{ \left[\exp(6K + 4H/3) + \exp(H/3) [\cosh(2\Delta_+) - \alpha_+/\Delta_+ \right. \right. \\
 & \times \left. \sinh(2\Delta_+) \right] / [2 \exp(2K) \cosh(2H/3)] \\
 & \times \left\{ \exp(6K - 4H/3) + \exp(-H/3) [\cosh(2\Delta_+) \right. \\
 & \left. \left. + \alpha_+/\Delta_+ \sinh(2\Delta_+)] + \exp(-H/3) [\cosh(2\Delta_-) + \alpha_-/\Delta_- \sinh(2\Delta_-)] \right\} \right\} \\
 & \quad \quad \quad (14b)
 \end{aligned}$$

$$\begin{aligned}
 H' = \frac{3}{2} \ln & \left\{ \left[\exp(6K + 4H/3) + \exp(H/3) [\cosh(2\Delta_+) - \alpha_+/\Delta_+ \sinh(2\Delta_+)] \right] \right. \\
 & \left. / \left[\exp(6K - 4H/3) + \exp(-H/3) [\cosh(2\Delta_-) - \alpha_-/\Delta_- \sinh(2\Delta_-)] \right] \right\} \\
 & \quad \quad \quad (14c)
 \end{aligned}$$

and

$$C' = 4C + 6W' + 3K' + 3 \ln[2 \cosh(2H/3)] \quad (14d)$$

where $\alpha_{\pm} = \pm H/6 + K$ and $\Delta_{\pm} = (H^2/36 \pm KH/3 + K^2 + 8W^2)^{1/2}$. This completes the renormalisation group transformation. When the external magnetic field vanishes, we recover the decimation results for the isotropic Heisenberg model [15] (with $K \rightarrow 2K$)

$$\exp(4K') = (2 \exp(4K) + \exp(-8K))/3. \quad (15)$$

We should make clear that the method described above could also be used for the one-dimensional and three-dimensional cases. For hypercubic lattices the bond-moving step combines 2^{d-1} bonds in parallel. Critical properties of the diluted Heisenberg model without field in one, two and three dimensions were studied by similar methods by Stinchcombe [15].

In zero magnetic field our recursion relations are similar to those obtained in [14] and consequently our phase diagram is the same as that shown in figure 6 of [14]. The system displays a phase transition at a finite temperature only for the anisotropic case ($\Delta \neq 0$). For the isotropic case the phase transition occurs at $T = 0$ and is associated with a strong-coupling fixed point at $W = K = \infty$.

The recursion relations for $H \neq 0$ are in agreement with the expected behaviour of the anisotropic Heisenberg ferromagnet in the presence of an external magnetic field, i.e. the system exhibits no phase transition. In the isotropic case, for $H = 0$, the flow is towards the attractor at $K = 0$; however, for $H \neq 0$ the recursion relations flow to $W = 0, K/W = \infty, H = \pm \infty$. In other words, even if we start with an isotropic situation ($\Delta = 0$), the magnetic field induces an anisotropy and the system in an applied external field flows to the Ising attractor at $K/W = \infty, H = \pm \infty$.

To obtain the critical behaviour of the Heisenberg ferromagnet at very low temperatures, we expand the renormalisation group equations close to the isotropic strong-coupling fixed point $W = \infty, W/K = 1$ and $H/W \ll 1$, to obtain ($H/6K > \Delta$)

$$W_{n+1} = b^a W_n - C_0 W_n \Delta_n - C_1 H_n + C_2 \quad (16a)$$

$$H_{n+1} = b^r H_n + C_3 W_n \Delta_n \quad (16b)$$

$$W_{n+1} \Delta_{n+1} = b^s W_n \Delta_n + O(H_n^2) \quad (16c)$$

where $b = 2$ is the scaling factor, $a = 0$ as expected since $d = 2$ is the lower critical dimension for the Heisenberg ferromagnet, implying that the fixed point at $W = \infty$ is marginal. This marginality gives rise to exponential temperature dependences for the

physical quantities at very low temperatures as we show below. The constants are $C_0 = \frac{1}{3}$, $C_1 = \frac{1}{18}$ and $C_2 = \frac{1}{4} \ln(\frac{2}{3})$. The exponent $r = 1.41$ instead of $r = d = 2$ as expected from general arguments [16] at least for Ising systems. The exponent $s = \ln(\frac{4}{3})/\ln(2)$. It is interesting to point out that, when we carry out a similar expansion in the presence of a small anisotropy and for a magnetic field satisfying the condition $1 \gg \Delta > H/6K$, we obtain $H_{n+1} = 4H_n$ showing that, when the rotational symmetry of the Hamiltonian is broken, the magnetic field at $T = 0$ scales as b^d .

We start iterating the equations above with $\Delta_0 = 0$, $W_0 = W/C_2$ and $H_0 = H(H/W \ll 1)$ and, since the anisotropy Δ remains zero to linear order in the magnetic field, we shall consider these equations with $\Delta = 0$. In this case they can be iterated to a length scale $l = b^n$, and in the limit $a \rightarrow 0$ they yield

$$W_l = W_0 - (\ln l)/(\ln b) - C[(1 - l^r)/(1 - b^r)]H_0 \quad (17)$$

where $W_0 = (1/C_2)(J/2k_B T)$, $C = C_1/C_2$, $b = 2$ and $H_0 = \mu B_0/k_B T$. Let us first consider the case $H = 0$. Iterating to $W_l = 0$, we obtain the correlation length $\xi \propto \exp(gJ/2k_B T)$ where $g = (\frac{1}{2} \ln 2)/C_2 \approx 3.42$. The correlation length diverges exponentially as the $T = 0$ transition is approached. For large magnetic fields we get $\xi \propto (W/H)^{1/r}$. The crossover field H_c is therefore given by

$$H_c = W \exp(-gW/r). \quad (18)$$

This expression determines the form in which the magnetic field, at $T \neq 0$, appears in the scaling functions for the different thermodynamic quantities, i.e. as H/H_c or $(H/W) \exp[(g/r)(J/2k_B T)]$. Since the crossover line rises exponentially we expect to observe important field effects at very low temperatures even in small fields.

The exponential temperature dependence that we derived explicitly for the correlation length also shows up in the susceptibility [17] and gives rise to strong divergencies in the low-temperature magnetisation as discussed below.

An important characteristic of systems exhibiting a zero-temperature phase transition is their anomalous dynamics which is associated with a breakdown of conventional critical slowing down [18]. MacMillan [19] has proposed a relation between the energy barrier for relaxation of a cluster of size l and the coupling constant at the same length scale: $\vartheta_{n+1} = W_n + \vartheta_n$ with $\vartheta_0 = 0$ since there is no barrier for flipping a spin, and such that the relaxation time $\tau_l \propto \exp(\vartheta_l)$. Iterating this equation we get $\vartheta_N = V_N/T = \sum_{n=0}^N W_n$ which together with the recursion relation for the coupling constant in zero field yields

$$\tau_\xi \propto \exp(\vartheta_\xi) = \tau_0 \exp[\alpha(J/2k_B T)^2] \quad (19)$$

where $\alpha = (1/C_2)^2$ and $(1/\tau_0) = J/\hbar$.

We expect this extreme slowing down of the critical fluctuations to give rise to non-equilibrium effects at very low temperatures as the transition is approached.

4. Magnetisation calculations

With general renormalisation group equations such as equations (14), it is possible to study the phase diagram and to obtain critical exponents; however, we need some extra consideration in order to calculate the thermodynamic functions. We show now how to obtain the magnetisation.

For a crystal of N sites, the magnetisation per spin is defined as

$$m = \mu_{\text{sat}} \langle \sigma_i^z \rangle = \mu_{\text{sat}} (1/N) (1/Z_N) \text{Tr}[\sigma_i^z \exp(\mathcal{H})] \quad (20)$$

where $Z_N \equiv \text{Tr}[\exp(\mathcal{H})]$ is the partition function and \mathcal{H} is a reduced Hamiltonian as in equation (1). The choice of the site (or Bravais indices) i is irrelevant owing to the lattice translational symmetry. When the system is embedded in an external magnetic field B_0 , the above trace can be written as

$$m_H \equiv \langle \sigma_i^z \rangle = (1/N) (\partial/\partial H) [\ln(Z_N)]. \quad (21)$$

Let us now generalise the thermodynamic densities used to characterise thermodynamic phase coexistence [16], to deal with a magnetic quantum system. The general magnetisation associated with the coupling constant K is given by the following trace:

$$m_K \equiv (1/Z_N) \text{Tr}[\sigma_i^z \sigma_j^z \exp(\mathcal{H})] \quad (22)$$

which can also be written as

$$m_K = (1/N_p) (\partial/\partial K) [\ln(Z_N)] \quad (23)$$

where N_p is the number of bonds ($N_p = 3N$ for the two-dimensional triangular lattice). Similarly we introduce the general magnetisation associated with W ($m_W = \langle \sigma_i^x \sigma_j^x + \sigma_i^y \sigma_j^y \rangle$) and that associated with the constant C which is the trace of the identity matrix. Using a compact notation ($J_0 \equiv C$, $J_1 \equiv K$, $J_2 \equiv W$ and $J_3 \equiv H$), we can write

$$m_\alpha = (1/N_x) [\partial(\ln Z_N)/\partial J'_\beta] (\partial J'_\beta/\partial J_\alpha) \quad (24a)$$

or

$$m_\alpha = (1/b^d N'_x) [\partial \ln Z_{N'}] / \partial J'_\beta T_{\alpha\beta} = b^{-d} m'_\beta T_{\alpha\beta} \quad (24b)$$

where the summation convention is used, $N_x = N$ or N_p , and the invariance of the partition function under renormalisation, namely $Z_N = Z_{N'}$, has also been used. In general, $Z_N = Z_{N'}$ only when a constant in the Hamiltonian is carried out upon renormalisation.

If we want to determine the magnetisation m at any point (K, W, H) in the global phase diagram, we need to study the flow from such point to the attractor (sink) which dominates the region. Physical considerations are used to estimate the generalised magnetisations in the neighbourhood of the sink. Then the generalised magnetisations are followed back, via equation (24b), to the original (K, W, H) point.

Our method resembles the method to obtain recursively the free energy for an Ising system introduced by Nauemberg and Nienhuis [20] and generalised later [21]. Here we incorporate the constant in the Hamiltonian and it is treated as a coupling constant.

5. Application to adsorbed solid ^3He

Godfrin *et al* [7, 11] have made a detailed study of adsorbed ^3He magnetisation. A NMR spectrometer was used to measure the ^3He absorption lines at 461 kHz (corresponding to an applied magnetic field $B_0 = 14.21$ mT) and 209 kHz ($B_0 = 6.44$ mT). Based on previous measurements [8, 9], they worked at a ^3He coverage near the middle of second-layer completion where the largest ferromagnetic effects of the film arise. At lower densities, up to first-layer completion, the system behaves as free spins and follows

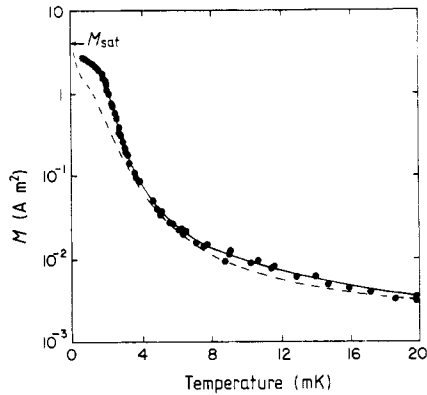


Figure 1. Total magnetic moment vs. temperature: ●, experimental measurements for $B_0 = 14.21$ mT as in [7]; —, is a ten-term high-temperatures expansion ($J = 2.1$ mK); ---, renormalisation group results ($J = 2.1$ mK; $B_0 = 14.21$ mT).

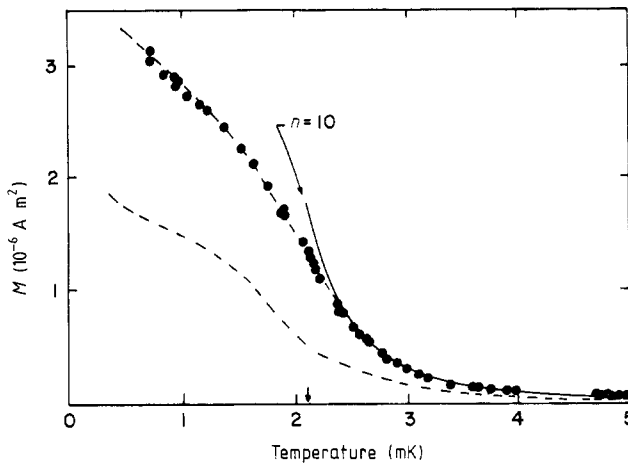


Figure 2. The same as figure 1 but for low-temperature results.

close to a Curie law. The magnetisation deviates from a factor of about 1.7 at higher temperatures (20–24 mK) to a factor of 10^2 at low temperatures (about 1 mK) with respect to the free-spin value. To interpret these data they assumed a two-dimensional nearest-neighbour ferromagnetic $S = \frac{1}{2}$ Heisenberg Hamiltonian to describe the second-layer magnetism. The high-temperatures series expansion in the parameter $K = J/2k_B T$ up to ten terms was used and it described well the data with $J = 2.1$ mK. These features are reproduced here in figures 1–3. The agreement is excellent for $T > 2.1$ mK, the region of validity of such expansion.

Our calculations are performed along a straight line in the K, W, H space, with $K = W$ (isotropic case) determined by the K/H ratio. As in [7, 11], we use $J = 2.1$ mK and $\mu = 0.78$ mK T^{-1} for the ^3He magnetic moment. Thus, different applied fields correspond to different straight lines and the various points on one line correspond to different temperatures. Since there is no phase transition at finite temperatures, all relevant points flow to the attractor with $W = 0, K/W = \infty, H = +\infty$ (for $H = 0$ the flow is towards $K = W = H = 0$). The magnetisation per spin in the neighbourhood of the attractor is equal to unity.

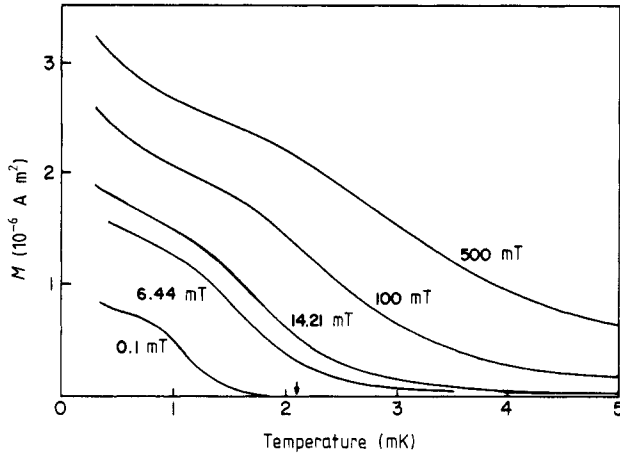


Figure 3. The magnetisation of the ^3He layer for various applied magnetic fields.

In figure 1 we compare our renormalisation group calculations with the magnetisation measurements and high-temperature expansion for the case with applied magnetic field of 14.21 mT. We used here the saturation magnetisations for the ^3He layer of $4.3 \times 10^{-6} \text{ A m}^2$. Above 3 mK our results are in excellent agreement with the experimental data and below they are systematically lower than the data. At $T \gg J$ we also obtain a Curie behaviour with a Curie constant of $5.78 \times 10^{-11} \text{ K A m}^2$.

In figure 2 we show the details of the low-temperature values for the magnetisation. Our values are systematically below the experimental values. The difference increases below $T \approx J$ (where the ferromagnetic coupling becomes important). We point out that our finite-cell renormalisation does not incorporate low-energy excitations such as long-wavelength spin waves. In the absence of a magnetic field this should restrict our analysis to temperatures $T \geq J$. This is shown clearly in the calculation for the specific heat as discussed below and which rises exponentially at low temperatures. In the presence of an external magnetic field the dramatic effect of the field is evidenced for example through the behaviour of the correlation length in zero and finite field as discussed in section 3. In this case ($B_0 \neq 0$) we expect our approach to give a correct description of the system also in the region of field-dominated behaviour, above the crossover line, i.e. for $T < T_c = (gJ)^{-1} \ln(H/W)$. It is interesting that, although our method does not take into account low-frequency excitations, our magnetisation falls substantially below the experimental results at very low temperatures. This may indicate the existence of finite size effects, and interplane coupling in the ^3He system. Near $T = 1.5 \text{ K}$ there is an inflection point which is caused by the crossover between temperature- and magnetic-field-dominated regions. In section 3 we derived an expression for the crossover field H_c which predicts two distinct behaviours for the thermodynamic functions. For a magnetic field of 14.21 mT the crossover is at 1.3 mK and therefore we expect a singular behaviour around this temperature. In figure 3 we plot various magnetisation curves for different magnetic fields and our equation (18) for the crossover field works well, indicating where the change in concavity must occur. For instance at a field of 100 mT the crossover is around 2 mK as can be easily seen in the figure. This behaviour cannot be ruled out by the experimental data of [7, 11] even though it is not so sharp as in our pictures. The quantitative differences may be attributed to interplane interactions which

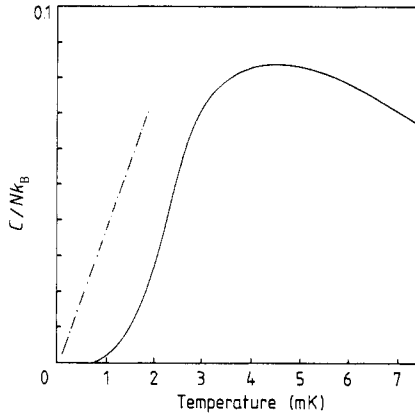


Figure 4. The specific heat as a function of temperature: —, calculated from the average cell energy; - · -, from the low-temperature recursion relation expansion.

enhances the interparticle and magnetic couplings or to our small-cell method. The use of larger cells will certainly give more accurate results.

We calculate the specific heat by two methods: we first note that the average energy per bond ($B_0 = 0$) is $K(m_K + m_W)$ and therefore we can easily obtain the specific heat as function of temperature. The result is shown in figure 4 by the full curve. We immediately see that the low-temperature behaviour resembles more that of a system with finite levels than a Heisenberg system. This is because a small number of Heisenberg spins have finite levels and therefore an exponential specific heat at low temperatures. This behaviour was also found by Bonner and Fisher [22] in dealing with the one-dimensional finite Heisenberg chain. We have also calculated the specific heat using the result (equation (16)) for the coupling strength at a length scale l together with the expression [17]

$$C_V = T \frac{\partial S}{\partial T} = T \frac{\partial}{\partial T} \left(d \int_1^{\xi} \frac{dl}{W_l l^{d+1}} \right)$$

to obtain a linear temperature dependence for C_V at very low temperatures ($T \ll J$) as shown in figure 4. This result which is based on the general form of the recursion relation is independent of the length scale factor b and incorporates all length scales, providing a better description of the low-temperature thermodynamic behaviour. The specific heat maximum around $T = 3$ mK is above the experimental result that indicates a maximum around $T = 2$ mK [11].

Finally, we point out that equation (19) for the critical slowing down predicts relaxation times of order 10^{-4} s, 10 s and 10^{35} s for temperatures 1.0 mK, 0.5 mK and 0.1 mK, respectively. Since the time constant for the magnetisation measurements are of the order of 1 min, we predict that 'glassy' effects will show up for measurements below 0.5 mK.

6. Conclusions

We have developed a quantum mechanical renormalisation group formalism to treat the nearest-neighbour $S = \frac{1}{2}$ Heisenberg model in the presence of an external magnetic

field. We have also derived a general method to calculate recursively the magnetisation which enables direct comparison with experimental measurements. Our procedure based on a $b = 2$ Migdal–Kadanoff method was worked out in detail and applied to this novel two-dimensional Heisenberg ferromagnet consisting of a solid ^3He adsorbed layer. The study of the dynamics of the system predicted very large relaxation times for temperatures below 0.5 mK in very small external fields. The analysis of the renormalisation group recursion relations yielded a crossover behaviour around 1.3 mK for the external magnetic fields used in the experiments. The results are encouraging since for $T > J$ we obtained good quantitative agreement and qualitative agreement for temperatures above the crossover temperature. It is also possible that the low-temperature data might be under the influence of interplane mechanisms. As suggested [11], preplating the substrate with ^4He should help to explain this question. However, new renormalisation group analysis based on computer simulations [23] seems to endorse the experimental results for the magnetisation.

As we have discussed, in order to improve upon the quantitative results we have to consider large arrays such as the $b = 3$ case which is under study now.

Acknowledgments

We benefited from discussions with Professor R Rapp and Professor H Godfrin. We also thank H Godfrin for bringing [23] to our attention and the Brazilian National Council of Scientific and Technological Development (CNPq) for partial financial support.

References

- [1] Cross M C and Fisher D S 1985 *Rev. Mod. Phys.* **57** 881
- [2] Ahonen A I, Kodama T, Krusius M, Paalanen M A, Richardson R C, Schoepe W and Takano Y 1976 *J. Phys. C: Solid State Phys.* **9** 1665
- [3] Godfrin H, Frossati G, Thoulouze D, Chapellier M and Clark W G 1978 *J. Physique Coll.* **39** C6 2871
- [4] Bozler H M, Bartolac T, Luly K and Thomson A L 1978 *Phys. Rev. Lett.* **41** 490
- [5] Dash J G 1975 *Films on Solid Surfaces* (New York: Academic)
- [6] Sciver S W and Vilches O E 1978 *Phys. Rev. B* **18** 285
- [7] Godfrin H, Ruel R R and Osheroff D D 1988 *Phys. Rev. Lett.* **60** 305
- [8] Franco H, Rapp R E and Godfrin H 1986 *Phys. Rev. Lett.* **57** 1161
- [9] Franco H, Godfrin H and Thoulouze D 1985 *Phys. Rev. B* **31** 1699
- [10] Roger M and Delrieu J M 1987 *Japan. J. Appl. Phys.* **26** 267
- [11] Godfrin H, Ruel R R and Osheroff D D 1988 *J. Physique Coll.* C8 2045
- [12] Caride A O, Tsallis C and Zanette S I 1983 *Phys. Rev. Lett.* **51** 145
- [13] Takano H and Susuki M 1981 *J. Stat. Phys.* **26** 635
- [14] Mariz A M, Tsallis C and Caride A O 1985 *J. Phys. C: Solid State Phys.* **18** 4189
- [15] Stinchcombe R B 1975 *J. Phys. C: Solid State Phys.* **12** 4533
- [16] Fisher M E and Berker A N 1982 *Phys. Rev. B* **26** 2507
- [17] Takahashi M 1987 *Phys. Rev. Lett.* **58** 168
- [18] Rammal R 1985 *J. Physique* **46** 1837
- [19] MacMillan W L 1984 *J. Phys. C: Solid State Phys.* **7** 3179
- [20] Nauenberg M and Nienhuis B 1975 *Phys. Rev. Lett.* **35** 477
- [21] Niemeijer Th and van Leeuwen J M J 1976 *Phase Transitions and Critical Phenomena* vol 5 (New York: Academic) ch 7
- [22] Bonner J C and Fisher M E 1964 *Phys. Rev.* **135A** 640
- [23] Kopietz P, Scharf P, Skaf M S and Chakravarty S 1989 *Europhys. Lett.* **9** 465